國立臺灣大學生命科學院生命科學系

碩士論文

Department of Life Science

College of Life Science

National Taiwan University

Master's Thesis

四氫皮質酮和其異構體對於神經母細胞瘤治療之研究

Investigating the Effect of Tetrahydrocorticosterone and Its Isomers on Neuroblastoma Treatment

虞智凱

Zhi-Kai Yu

指導教授：李心予 博士

Advisor: Hsinyu Lee, Ph.D.

中華民國 114 年 5 月

May 2025

doi:10.6342/NTU202501007

國立臺灣大學碩士學位論文
口試委員會審定書
MASTER'S THESIS ACCEPTANCE CERTIFICATE
NATIONAL TAIWAN UNIVERSITY

四氫皮質酮和其異構體對於神經母細胞瘤治療之研究

Investigating the Effect of Tetrahydrocorticosterone and Its Isomers on Neuroblastoma Treatment

本論文係 虞智凱 R11b21032 在國立臺灣大學生命科學系完成之碩士學位論文，於民國 113 年 5 月 7 日承下列考試委員審查通過及口試及格，特此證明。

The undersigned, appointed by the Department of Life Science on 7th May 5, 2025 have examined a Master's Thesis entitled above presented by Zhi-Kai Yu R11b21032 candidate and hereby certify that it is worthy of acceptance.

口試委員 Oral examination committee:

李心予　許文明　陳永盛

（指導教授 Advisor）

余沛諭

系（所、學位學程）主管 Director: 鄭貽生

doi:10.6342/NTU202501007

誌謝

在碩士生涯即將告一段落之際，回首這段充實而深具意義的時光，心中滿懷感激。首先，要感謝李心予老師讓我進到實驗室學習與成長。老師在學術領域的專業引領，以及我在人生與研究方向上迷惘時所給予的指導與陪伴，都是我這段旅程中最重要的支柱。無論是技術上的指導還是經驗的分享，老師總是毫不保留，讓我得以逐步建立起屬於自己的研究節奏與信心。在這段歷程中，我不僅習得實務操作的能力，也培養出作為一位科學研究者所需的邏輯與思維，這些收穫將成為我未來道路上的寶貴養分。

特別感謝吳沛翊老師，在教學與研究事務繁忙之餘，仍不吝抽空關心我的進度，並經常與我討論實驗設計與結果，不僅提供了專業建議，更給予我莫大的支持與鼓勵。感謝許文明醫師與廖永豐老師擔任口試委員，對論文內容給予寶貴的建議，使我的研究更加完善與成熟。實驗室生活中，能與一群真誠又互相扶持的夥伴共度時光，是我在研究壓力下的重要依靠。無論是在學術討論、技術互助或生活交流上，祥嫚、晏慈、俊逖、貫浤等人始終給予我許多溫暖與動力。雖然俊逖最終選擇轉換發展方向，仍由衷祝福未來順利、前程似錦。奕勳是我剛進實驗室時的重要引路人，謝謝你當時毫不保留地教我技術、分享經驗，也給了我很多信心。還有彩珊，在進行動物實驗時，不僅從零開始耐心教我流程與技巧，也協助我克服多次困難，助我順利完成研究任務。對於曾經提供建議、協助修改論文草稿與分享經驗的所有師長與前輩，我亦銘記於心。

而我最深的謝意，留給一直以來支持我、陪伴我成長的家人。謝謝爸爸、媽媽與妹妹一路上的陪伴與支持，無論我選擇什麼樣的道路，你們始終無條件地相信我、支持我，使我得以無後顧之憂。這段碩士旅程之所以得以完成，離不開所有人的幫助與鼓勵。衷心向每一位在這段路途中伸出援手的人致意，感謝你們豐富了我的生命篇章。

doi:10.6342/NTU202501007

中文摘要

神經母細胞瘤是嬰兒期最常見的顱外實體腫瘤，起源於胚胎發育期間神經脊細胞的異常增生，通常發生於與交感神經系統相關的區域。芳香烴接受器（Aryl hydrocarbon receptor, AHR）為一種配體活化的轉錄因子，已知能促進神經母細胞瘤細胞的分化。四氫皮質酮（Tetrahydrocorticosterone, THB）作為一種內源性糖皮質激素，近期被鑑定為可活化 AHR 的內源性配體，並能調控斑馬魚的神經生成與神經分化。此外，一種結構上與 THB 相似的合成化合物，稱為 Compound Y，亦已被開發。基於上述發現，本研究假設 Compound Y 與 THB 可透過活化 AHR，促進神經母細胞瘤細胞分化，進而抑制其增生。在本研究中，Compound Y 與 THB 皆可有效抑制神經母細胞瘤細胞的增生，並提升神經分化標誌物，包括生長相關蛋白 43（GAP43）與神經元特異性烯醇酶（NSE）的表現。此外，本研究亦建立一套以 GAP43 啟動子活性為基礎的螢光酶篩選平台，以加速分化促進劑的篩選流程。利用來自 TH-MYCN 轉基因小鼠的原代神經母細胞瘤細胞進行體外實驗，進一步確認 Compound Y 具有抑制細胞增生的作用。體內分析亦顯示，Compound Y 能顯著延緩腫瘤進展並延長 TH-MYCN 小鼠的存活時間。綜合以上結果，Compound Y 與 THB 具備透過 AHR 介導的分化機制治療神經母細胞瘤的潛力，為未來的治療策略提供重要依據。

關鍵字：四氫皮質酮、芳香烴接受器、神經分化、神經母細胞瘤、TH-MYCN 轉基因小鼠

doi:10.6342/NTU202501007

Abstract

Neuroblastoma is the most common extracranial solid tumor in infancy, originating from aberrant proliferation of neural crest cells during embryonic development and typically arising in regions associated with the sympathetic nervous system. The aryl hydrocarbon receptor (AHR), a ligand-activated transcription factor, has been shown to promote the differentiation of neuroblastoma cells. Tetrahydrocorticosterone (THB), a glucocorticoid, was recently identified as an endogenous AHR activator that regulates neurogenesis and neural differentiation in zebrafish. In addition, a synthetic compound structurally similar to THB, referred to as Compound Y, has been developed. Based on these findings, it was hypothesized that both Compound Y and THB promote neuroblastoma cell differentiation through AHR activation, thereby inhibiting cell proliferation. In this study, both Compound Y and THB were demonstrated to inhibit neuroblastoma cell proliferation while enhancing the expression of neural differentiation markers, including growth-associated protein 43 (GAP43) and neuron-specific enolase (NSE). To facilitate efficient identification of differentiation-inducing compounds, a luciferase-based screening platform targeting GAP43 promoter activity was established. Additionally, *ex vivo* experiments using primary neuroblastoma cells derived from TH-MYCN transgenic mice confirmed the growth-inhibitory effects of Compound Y. *In vivo*

doi:10.6342/NTU202501007

analysis further demonstrated that Compound Y significantly slowed tumor progression and prolonged survival in TH-MYCN mice. Collectively, these findings highlight the therapeutic potential of Compound Y and THB in neuroblastoma treatment by targeting AHR-mediated differentiation pathways.

Keywords: Tetrahydrocorticosterone; Aryl hydrocarbon receptor; Neural differentiation; Neuroblastoma; TH-MYCN transgenic mice

doi:10.6342/NTU202501007

Table of Contents

doi:10.6342/NTU202501007

doi:10.6342/NTU202501007

List of Figures

doi:10.6342/NTU202501007

1. Introduction

1-1 Neuroblastoma

Neuroblastoma is the most commonly diagnosed pediatric cancer. It typically arises from genetic mutations in neural crest cells during early embryonic development, which disrupt the regulation of cell proliferation (Fig. A) [1]. Genes commonly associated with neuroblastoma include ALK, KIF1B, MYCN, and PHOX2B, as well as deletions in genes located on chromosomes 1 and 11. Familial neuroblastoma is extremely rare, accounting for only 1-2% of all cases [2].

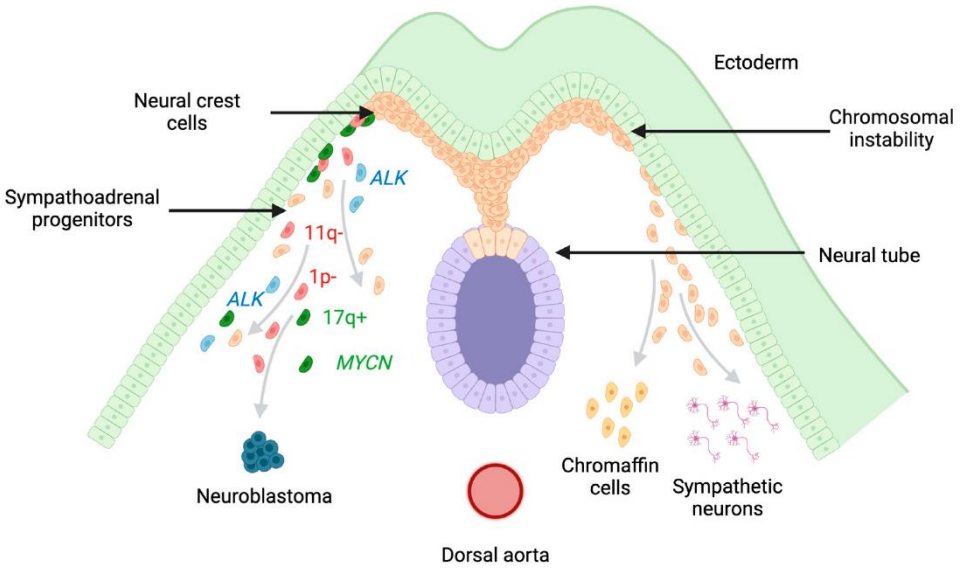

Figure A. Development of neuroblastoma from the neural crest [1].

During development, neural crest cells differentiate into components of the sympathetic nervous system. As a result, tumors can occur in any region where sympathetic nerves are present, with the adrenal glands being the most common site,

doi:10.6342/NTU202501007

followed by the neck, chest, abdomen (excluding the adrenal glands), spinal cord, and pelvis. Clinical presentations of neuroblastoma vary widely, ranging from spontaneous tumor regression to highly metastatic, undifferentiated tumors with poor prognoses. Consequently, neuroblastoma is recognized as a complex and highly heterogeneous disease.

Neuroblastoma accounts for approximately 7% of all pediatric cancers but is responsible for about 15% of childhood cancer-related deaths [3, 4]. The annual incidence rate among children aged 0 to 14 years is approximately 10.2 cases per million [5]. The disease often metastasizes before symptoms appear, resulting in approximately 50% of cases being diagnosed at intermediate- or high-risk stages [6]. While the long-term survival rate for low-risk patients exceeds 90%, the five-year overall survival rate for high-risk patients remains below 50%, even with intensive treatment [7]. Treatment failure and relapse in high-risk patients continue to be major contributors to pediatric cancer mortality.

The International Neuroblastoma Staging System (INSS) was the first globally recognized standard for staging neuroblastoma. It classifies the disease into stages 1, 2A, 2B, 3, 4, and 4S based on the tumor's anatomical location and extent of spread at diagnosis. Stage 4 indicates widespread metastasis, a common characteristic of advanced cancers. Stage 4S, however, is a unique category that describes patients

doi:10.6342/NTU202501007

younger than one year of age with limited metastasis to specific organs—namely, the bone marrow, liver, or skin. Notably, the prognosis for Stage 4S is generally favorable, and in some cases, monitoring alone may be sufficient without additional treatment.

More recently, a new classification system—the International Neuroblastoma Risk Group Staging System (INRGSS)—has been proposed. Unlike the INSS, which is based on surgical and pathological findings, the INRGSS is a pre-treatment clinical staging system that relies on imaging studies to evaluate tumors and identify image-defined risk factors (IDRFs) (Fig. B) [8]. The key distinction between the two systems lies in their timing and criteria: while the INSS staging is determined post-surgically, the INRGSS stratifies patients before treatment based on clinical and biological markers, including age at diagnosis, tumor stage, histological differentiation, MYCN gene amplification, deletion of chromosome 11q, and tumor cell ploidy. Based on these factors, patients are assigned to very low-, low-, intermediate-, or high-risk groups, each receiving stratified treatment strategies according to risk level prior to surgical intervention.

doi:10.6342/NTU202501007

INRG Stage	Age (months)	Histologic Category	Grade of Tumor Differentiation	*MYCN*	11q Aberration	Ploidy	Pretreatment Risk Group
L1/L2		GN maturing; GNB intermixed					A Very low
L1		Any, except GN maturing or GNB intermixed		NA			B Very low
				Amp			K High
L2	< 18	Any, except GN maturing or GNB intermixed		NA	No		D Low
					Yes		G Intermediate
	≥ 18	GNB nodular; neuroblastoma	Differentiating	NA	No		E Low
					Yes		H Intermediate
			Poorly differentiated or undifferentiated	NA			
				Amp			N High
M	< 18			NA		Hyperdiploid	F Low
	< 12			NA		Diploid	I Intermediate
	12 to < 18			NA		Diploid	J Intermediate
	< 18			Amp			O High
	≥ 18						P High
MS	< 18			NA	No		C Very low
					Yes		Q High
				Amp			R High

Figure B. International neuroblastoma risk group staging system [8].

Numerous therapeutic strategies are currently being developed for the treatment of neuroblastoma. Patients classified as low- or intermediate-risk, based on disease progression, generally have favorable prognoses and a high likelihood of being cured through conventional chemotherapy or surgical intervention. In contrast, high-risk patients typically exhibit lower survival rates and require a multimodal treatment approach, which may include chemotherapy, surgery, radiotherapy, hematopoietic stem cell transplantation, and differentiation therapy.

Differentiation therapy employs agents that promote the maturation of neuroblastoma cells into non-proliferative neural cells. One such agent is isotretinoin, a synthetic isomer of retinoic acid, which induces differentiation of neuroblastoma cells into mature neurons, leading to cell cycle arrest and apoptosis. Retinoic acid itself has

doi:10.6342/NTU202501007

also been shown to induce differentiation in undifferentiated neuroblastoma cells [9].

In recent years, immunotherapy has emerged as a promising strategy for neuroblastoma treatment. GD2, a disialoganglioside, is a glycolipid antigen highly expressed on the surface of neuroblastoma and other neuroectodermal tumor cells. Clinical studies have demonstrated that Dinutuximab—an anti-GD2 monoclonal antibody—combined with granulocyte-macrophage colony-stimulating factor (GM-CSF), interleukin-2 (IL-2), and retinoic acid, significantly improves short-term survival in patients with high-risk neuroblastoma [10].

MYCN amplification is among the most widely recognized genetic alterations in neuroblastoma, occurring in approximately 25% of all cases and in up to 40% of patients with advanced-stage disease [11, 12]. MYCN expression is positively associated with the activation of genes that promote tumor aggressiveness and malignancy [13]. Knockdown of MYCN expression has been shown to induce neural differentiation and apoptosis in neuroblastoma cells [14]. Patients with normal *MYCN* gene expression typically have a more favorable prognosis, while those exhibiting *MYCN* amplification or overexpression are often associated with rapid disease progression and higher mortality rates. Consequently, *MYCN* amplification is recognized as a critical prognostic marker of poor clinical outcomes and represents a promising therapeutic target in neuroblastoma.

doi:10.6342/NTU202501007

1-2 Aryl hydrocarbon receptor

Our previous study demonstrated that the expression of the aryl hydrocarbon receptor (AHR) is inversely correlated with MYCN levels in neuroblastoma tumors [15]. AHR belongs to the basic helix-loop-helix (bHLH) Per-ARNT-Sim (PAS) family and is the only member known to be ligand-activated [16]. It is best known for its role in mediating the toxic effects of 2,3,7,8-tetrachlorodibenzo-p-dioxin (TCDD), one of the most toxic exogenous environmental dioxins.

The molecular mechanisms underlying AHR signaling have been extensively studied. In its inactive state, AHR is bound to a cytoplasmic chaperone complex composed of heat shock protein 90 (Hsp90), prostaglandin E synthase 3 (p23), and co-chaperones such as X-associated protein 2 (XAP2, also known as AIP or ARA9) [17, 18]. Upon ligand binding, AHR undergoes a conformational change that disrupts its interaction with XAP2 and activates its nuclear localization signal (NLS), allowing AHR to translocate into the nucleus via the nuclear pore complex. Once in the nucleus, AHR dissociates from the chaperone complex and forms a heterodimer with the aryl hydrocarbon receptor nuclear translocator (ARNT, also known as HIF1β). This complex, along with additional cofactors, binds to xenobiotic response elements (XREs; consensus sequence CACGCNA/T) and the TATA box within the promoter region of target genes. Following transcriptional activation, AHR dissociates from ARNT and is

doi:10.6342/NTU202501007

exported back to the cytoplasm via CRM1 (exportin 1), where it rebinds to Hsp90 and completes the signaling cycle (Fig. C) [19, 20].

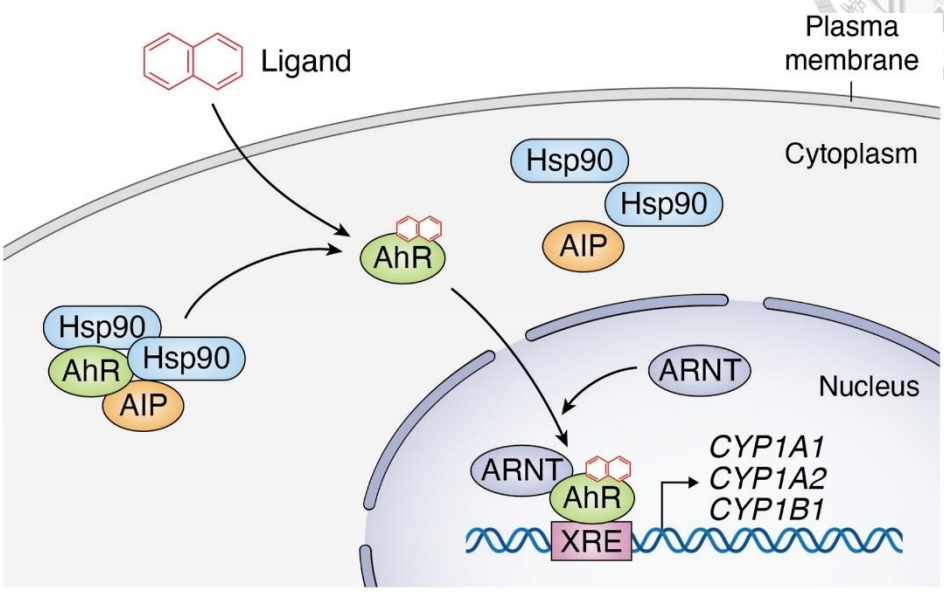

Figure C. Canonical AHR signaling pathway. In its inactive state, AHR is localized in the cytoplasm in complex with AIP and Hsp90. Ligand binding induces a conformational change, leading to dissociation from chaperone proteins and nuclear translocation, where AHR associates with ARNT and binds to XREs to activate target gene transcription [20].

AHR is a ligand-dependent transcription factor that can be activated by a wide range of exogenous compounds, including polycyclic aromatic hydrocarbons (PAHs), benzimidazoles, and flavonoids. Upon activation, AHR translocates to the nucleus and regulates the expression of xenobiotic-metabolizing enzymes such as CYP1A1, CYP1A2, and CYP1B1, which play key roles in drug and toxin metabolism [21]. In addition to exogenous ligands, AHR is also activated by endogenous metabolites,

doi:10.6342/NTU202501007

including eicosanoids derived from arachidonic acid. These ligands can further regulate CYP1 family gene expression, impacting lipid metabolism and immune responses [22]. AHR also interacts with other transcriptional regulators such as nuclear factor erythroid 2-related factor 2 (Nrf2) to induce the expression of phase II detoxifying enzymes, including glutathione S-transferase (GST), thereby promoting the elimination of reactive intermediates and maintaining redox homeostasis [23]. Studies have shown that dioxin-mediated AHR activation leads to disturbances in lipid metabolism, gluconeogenesis, and the tricarboxylic acid (TCA) cycle, resulting in hepatotoxicity and metabolic disorders [24]. These findings highlight the critical role of AHR in metabolic dysfunctions induced by environmental toxins.

In addition to metabolic regulation, AHR plays an important role in immune modulation. Its activation influences the differentiation of helper T cells and regulatory T cells (Tregs) [25]. AHR is also broadly expressed in dendritic cells and macrophages, where its activation promotes the production of anti-inflammatory cytokines such as IL-10 and suppresses the expression of pro-inflammatory cytokines [26]. Moreover, Toll-like receptor (TLR) signaling induces AHR expression, and AHR functions as a negative regulator of TLR-mediated immune responses [26, 27]. In barrier organs such as the intestine, skin, and lungs, AHR is essential for maintaining mucosal immune homeostasis and protecting against pathogenic invasion [28]. Owing to these

doi:10.6342/NTU202501007

physiological functions, AHR is increasingly regarded as a potential immunoregulatory target in autoimmune diseases, including rheumatoid arthritis [29], multiple sclerosis, systemic lupus erythematosus [30], and type 1 diabetes [31].

Beyond immune regulation, AHR also participates in controlling cell survival and differentiation. AHR has been shown to bind E2F1 and suppress E2F1-induced apoptosis, thereby negatively regulating programmed cell death [32]. In acute myeloid leukemia cells, AHR activation inhibits cell migration and invasiveness [33]. In melanoma cells, AHR upregulates the cyclin-dependent kinase inhibitor p27, arresting cell cycle progression at the G1 phase [34]. In SK-N-SH human neuroblastoma cells, TCDD inhibits proliferation by inducing G1 phase arrest through AHR activation [35]. AHR is expressed in cerebellar granule neuron precursors (GNPs) during early postnatal development, suggesting a role in regulating neuroblast proliferation and differentiation [36, 37]. AHR-deficient mice exhibit impaired neuronal differentiation in the dentate gyrus [38]. Furthermore, overexpression of AHR has been shown to promote neural differentiation in neuroblastoma cells [19, 39], and its expression positively correlates with the degree of differentiation in neuroblastoma tumor tissues [15]. Collectively, these findings highlight the importance of AHR in neural development and support its therapeutic potential in neuroblastoma treatment.

Given that AHR is a ligand-activated receptor, pharmacological activation of AHR

doi:10.6342/NTU202501007

using specific agonists represents a promising strategy for neuroblastoma therapy. Kynurenine (Kyn), a tryptophan-derived metabolite, is an endogenous ligand for AHR [40]. Our previous study demonstrated that Kyn-mediated AHR activation significantly downregulates MYCN expression, leading to reduced cell proliferation and enhanced neural differentiation [41]. *In vivo*, Kyn also inhibits neuroblastoma metastasis by upregulating the metastasis suppressor gene *KiSS-1* [41]. These findings further emphasize the therapeutic potential of AHR signaling in neuroblastoma. However, the clinical applicability of Kyn is limited by its low efficacy; a concentration of 200 μM is required to achieve only a 30% reduction in cell proliferation *in vitro*. Although Kyn is an endogenous substance with low toxicity, its limited efficacy excludes its use as an ideal therapeutic agent. Therefore, identifying a more effective and safer AHR agonist has become a key objective in the development of novel AHR-targeted therapies for neuroblastoma.

1-3 Tetrahydrocorticosterone

Tetrahydrocorticosterone (THB) is a planar molecule characterized by its hydrophobic and lipophilic properties and is predicted to bind to the hydrophobic ligand-binding domain of AHR [42, 43]. Our laboratory has identified two endogenous isomers, 5α-tetrahydrocorticosterone (5α-THB) and 5β-tetrahydrocorticosterone (5β-

doi:10.6342/NTU202501007

THB), as potential AHR ligands using a cell-free bioassay designed to detect dioxin-like compounds [44]. These isomers are metabolites of corticosterone, enzymatically converted by 5α-reductase and 5β-reductase, respectively. Both 5α-THB and 5β-THB are present in the central nervous system (CNS) and are classified as neuroactive steroids [45-50]. Previous studies have demonstrated that THB induces AHR translocation from the cytoplasm to the nucleus and subsequently activates the transcription of the downstream target gene *CYP1A1*, confirming its ability to activate AHR signaling [51]. Additionally, an *in vivo* study in zebrafish has shown that THB-mediated AHR activation promotes neurogenesis and supports the differentiation of myelinating glial cells, particularly oligodendrocytes and Schwann cells [51]. Furthermore, THB has been shown to induce neuronal differentiation in neuroblastoma cells [51]. Collectively, these findings suggest that THB possesses therapeutic potential for the treatment of neuroblastoma by promoting cellular differentiation through the activation of AHR signaling.

doi:10.6342/NTU202501007

Rationale

The aryl hydrocarbon receptor (AHR) is a ligand-activated transcription factor known to play a role in the regulation of neuroblastoma cell differentiation. Previous studies have identified tetrahydrocorticosterone (THB) and Compound Y as endogenous and exogenous ligands of AHR, respectively. Notably, THB has been shown to activate AHR and modulate neural development in zebrafish. Despite these findings, the therapeutic potential of THB and Compound Y in promoting neuroblastoma cell differentiation and suppressing tumor proliferation remains unclear. Therefore, this study aims to investigate whether THB or Compound Y can induce differentiation and inhibit proliferation of neuroblastoma cells *in vitro*, *ex vivo*, and *in vivo*. The therapeutic efficacy of these compounds was evaluated using the TH-MYCN transgenic mouse model of neuroblastoma. Through this research, we seek to elucidate the potential of THB and Compound Y as differentiation-inducing therapeutic agents and to establish a novel strategy for the treatment of neuroblastoma.

doi:10.6342/NTU202501007

2. Materials and methods

2-1 Cell culture

Human neuroblastoma cell lines SK-N-SH and SK-N-BE were obtained from the American Type Culture Collection (ATCC) and cultured in Dulbecco's Modified Eagle Medium (DMEM; Gibco), supplemented with 10% fetal bovine serum (FBS; Thermo Fisher Scientific Hyclone, Waltham, MA, USA), 100 U/mL penicillin, and 100 U/mL streptomycin. Cells were maintained in a humidified incubator at 37 °C with 5% CO_2.

Primary neuroblastoma cells were cultured in a medium consisting of 50% Neurobasal medium (Gibco), 40% DMEM/F12 (Gibco), and 10% FBS, supplemented with B-27 minus vitamin A (Gibco), N-2 supplement (Gibco), 0.01 μg/mL epidermal growth factor (EGF; Gold Biotechnology), 0.02 μg/mL basic fibroblast growth factor (bFGF; Gold Biotechnology), and 25 μg/mL primocin (InvivoGen).

2-2 Chemical reagents

5β-Tetrahydrocorticosterone (5β-THB) was purchased from Toronto Research Chemicals (Toronto, Ontario, Canada) and dissolved in DMSO. Compound Y was obtained from RDD Lab, Inc. (Wugu District, New Taipei City, Taiwan) and dissolved in DMSO. Retinoic acid was purchased from Sigma-Aldrich and also dissolved in

doi:10.6342/NTU202501007

DMSO. For treatment, all compounds were diluted 1:1000 in DMEM supplemented with 2% FBS.

2-3 Cell viability assay

Cell viability was assessed using the Cell Counting Kit-8 (CCK-8; Dojindo, Kumamoto, Japan). SK-N-SH and SK-N-BE cells were seeded in 96-well plates at densities of 10,000 and 12,000 cells per well, respectively, and allowed to adhere for 24 hours. Cells were then treated with the indicated compound and incubated for 24, 72, or 120 hours. Subsequently, 10 μL of CCK-8 reagent was added to each well and incubated for 1 hour. Absorbance was measured at 450 nm using a SpectraMax i3X microplate reader (Molecular Devices) to determine cell viability.

2-4 Western blot

Cells were washed with cold phosphate-buffered saline (PBS), and total protein was extracted using RIPA buffer (150 mM NaCl, 1% NP-40, 0.5% sodium deoxycholate, 0.1% SDS, 50 mM Tris, pH 7.5) supplemented with 1% protease inhibitor cocktail (Merck Millipore, Billerica, MA, USA). Lysates were centrifuged at 14,000 rpm for 15 minutes at 4 °C. Protein concentrations were determined using the Pierce BCA Protein Assay Kit (Thermo Scientific). Samples were mixed with protein

doi:10.6342/NTU202501007

loading buffer containing 2-mercaptoethanol (2-ME), then boiled at 100 °C for 10 minutes.

Proteins were resolved by SDS-PAGE (10% resolving gel; 90 V for 70 minutes in 4% stacking gel and 130 V for 1.5 hours in the resolving gel), and transferred to polyvinylidene fluoride (PVDF) membranes (Millipore Sigma; 100 V for 90 minutes at 4 °C). Membranes were blocked with 5% bovine serum albumin (BSA; Millipore Sigma) in TBST for 1 hour at room temperature, then incubated overnight at 4 °C with primary antibodies diluted in TBST containing 1% BSA. After washing three times with TBST, membranes were incubated with horseradish peroxidase (HRP)-conjugated secondary antibodies for 1 hour at room temperature. Signal detection was performed using enhanced chemiluminescence (ECL) reagents (Advansta, Menlo Park, CA, USA) and visualized with the UVP ChemStudio Plus imaging system (Analytik Jena, Jena, Germany). Band intensities were quantified using VisionWorks software (Analytik Jena).

The primary antibodies used were as follows: mouse polyclonal anti-GAP43 (sc-17790, Santa Cruz Biotechnology), chicken polyclonal anti-NSE (AB9698, Merck Millipore), and rabbit anti-GAPDH (GTX100118, GeneTex).

doi:10.6342/NTU202501007

2-5 Plasmid construction and luciferase assay

The promoter region of the *GAP43* gene was amplified from cDNA derived from SK-N-SH cells using Phusion High-Fidelity DNA Polymerase (Thermo Fisher Scientific). The cDNA template was obtained from Promega (Madison, WI, USA). The amplified *GAP43* promoter was cloned into the pGL4.32[luc2P/RFP/NF-κB-RE/Hygro] vector (Promega) between the *Nhe I* and *Bgl II* restriction sites.

Plasmids were transfected into cells using Lipofectamine® 3000 (Invitrogen, Carlsbad, CA, USA). Luciferase activity was measured using the ONE-Glo™ Luciferase Assay System (Promega), and normalized to RFP intensity.

Primer sequences used for promoter amplification were as follows:

GAP43pro-forward-Nhe I: 5′-AAG CTA GCA AAT GGT CTT ATC AAT GGA G-3′

GAP43pro-reverse-Bgl II: 5′-AAA GAT CTA AGG TCC ACA GCT ATT G-3′

2-6 Bioinspired Nanodroplet Processing (BioNDP) platform

The BioNDP platform procedure was conducted as described in a previous study [52]. The chip was sterilized by ultraviolet irradiation for 10 minutes before use. Compound solutions at various concentrations were dispensed into designated wells using a custom liquid handling system (Versa 10 spotter, Aurora Instruments Ltd., Vancouver, Canada). Each droplet had a volume of 200 nL. After dispensing, chips were

doi:10.6342/NTU202501007

incubated at room temperature for 10 minutes to allow solvent evaporation and compound deposition. Subsequently, a 200 nL droplet containing 200 cells was dispensed into each well, and the chip was sealed with a polydimethylsiloxane (PDMS)-glass gasket. After 24 hours of incubation, cell viability was measured using the CellTiter-Glo® Luminescent Cell Viability Assay (Promega), following the manufacturer's instructions. Luminescence was captured using the UVP ChemStudio Plus system (Analytik Jena, Jena, Germany) and analyzed with VisionWorks software (Analytik Jena).

2-7 Primary tumor cells isolation

Primary tumor cells were isolated as previously described [53]. Fresh neuroblastoma tumors were harvested from TH-MYCN transgenic mice, washed with PBS containing 25 μg/mL primocin, and sliced into 1–3 mm fragments. Tissues were enzymatically dissociated using a tumor dissociation kit (Miltenyi Biotec) and processed with a gentleMACS™ Dissociator (RWD Life Science) following the manufacturer's protocol. The resulting suspension was filtered through a 70 μm cell strainer, and red blood cells were lysed with RBC lysis buffer (Gibco).

A two-step cell purification process was employed. First, a non-tumor cell depletion kit (Miltenyi Biotec) was used to remove tumor-associated stromal cells,

doi:10.6342/NTU202501007

including lymphocytes, fibroblasts, and endothelial cells. Second, GD2-positive neuroblastoma cells were isolated by incubating the suspension with a Biotin-GD2 antibody (BioLegend), followed by magnetic separation using a biotin targeting kit (Miltenyi Biotec), according to the manufacturer's instructions (Fig. D).

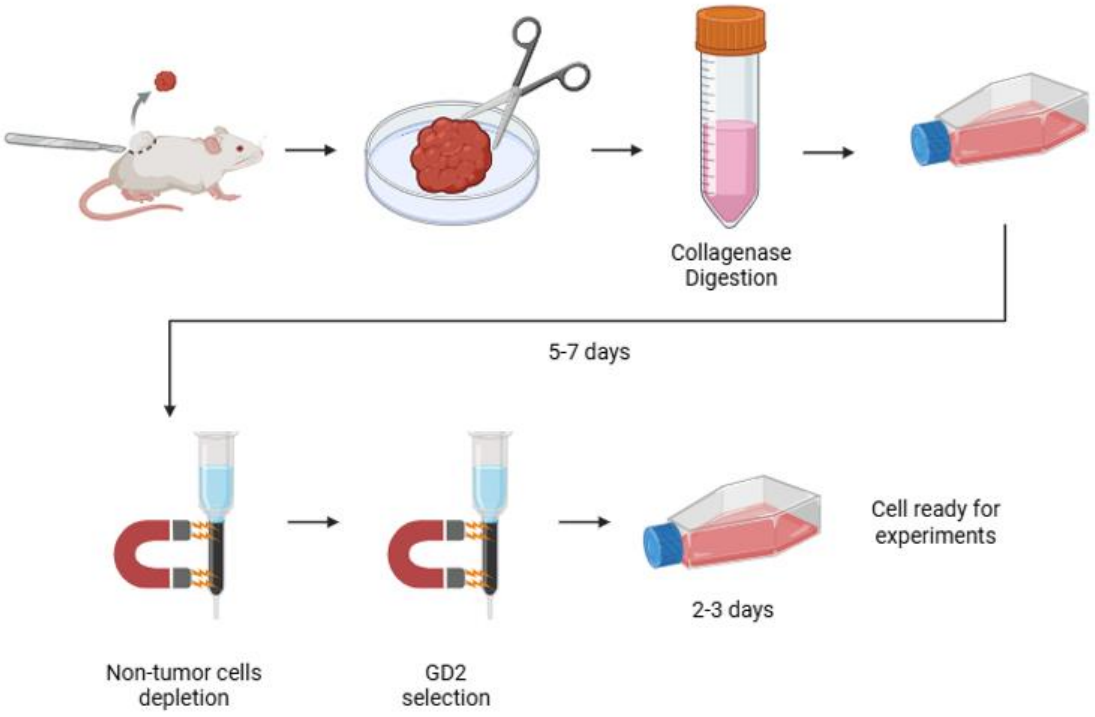

Figure D. General overview for primary neuroblastoma cell isolation.

2-8 Animal maintenance

The TH-MYCN transgenic mouse strain was maintained at the Transgenic Mouse Core Facility, College of Medicine, National Taiwan University. Following weaning, tumor development in hemizygous TH-MYCN mice was monitored weekly via ultrasound imaging in both axial and sagittal abdominal views. Mice were selected for

doi:10.6342/NTU202501007

treatment when tumor diameters exceeded 0.5 cm. Eligible mice were randomly assigned to treatment groups and received intraperitoneal injections of either vehicle (10% hydroxypropyl-β-cyclodextrin, Sigma-Aldrich) or 5 mg/kg of Compound Y. For the survival study, mice were euthanized via CO_2 inhalation when tumor diameter reached 1.5 cm.

Ultrasound imaging was performed using the PROSPECT ultrasound imaging system (Scintica, Canada). Mice were anesthetized with 1.5% isoflurane, and hair was removed from the abdominal and thoracic regions using a depilatory cream (Nair). During imaging, mice were positioned in a supine orientation on a stage coated with ultrasound transmission gel. The transducer was stereotactically lowered to contact the animal's skin surface. Tumors were identified as irregular or heterogeneous regions distinguishable from surrounding normal tissue landmarks. Tumor volume was calculated based on sonographic measurements of width, depth, and height, using a previously established formula [54].

2-9 Statistical analysis

All results are presented as the mean ± standard deviation (SD) from at least three independent experiments. Statistical comparisons among multiple groups were performed using one-way analysis of variance (ANOVA) in GraphPad Prism software

doi:10.6342/NTU202501007

(GraphPad Software, San Diego, CA, USA). Differences were considered statistically significant at $p < 0.05$ (*), $p < 0.01$ (**), and $p < 0.001$ (***).

doi:10.6342/NTU202501007

3. Results

3-1 Compound Y and THB inhibit neuroblastoma cell proliferation

Previous studies have suggested that the activation of AHR can promote the neural differentiation of neuroblastoma cells [15]. To assess the effects of Compound Y and THB on cell proliferation, a CCK-8 assay was performed on SK-N-SH cells. Results showed that Compound Y significantly inhibited SK-N-SH cell proliferation in a dose-dependent manner after 24 hours of treatment (Fig. 1A). In contrast, THB showed a significant inhibitory effect only after five days of treatment (Fig. 1B). In SK-N-BE cells, both Compound Y and THB significantly reduced cell proliferation in a dose-dependent manner (Fig. 1C–D). These findings suggest that both Compound Y and THB possess antiproliferative activity in neuroblastoma cells.

3-2 Compound Y and THB induce neuronal differentiation in neuroblastoma cells

To evaluate the differentiation-inducing effects of Compound Y and THB, neuroblastoma cells were treated with various concentrations of the compounds, and the expression levels of neuronal differentiation markers were assessed by Western blot analysis. Growth-associated protein 43 (GAP43) is known to play a critical role in axonal growth during neural development and regeneration [55], while neuron-specific

doi:10.6342/NTU202501007

enolase (NSE) is a marker of mature neurons that increases with differentiation [56]. In SK-N-SH cells, both Compound Y and THB elevated the expression of GAP43 (Fig. 2A), and high concentrations of Compound Y additionally increased NSE levels (Fig. 2B). Similarly, in SK-N-BE cells, both compounds enhanced GAP43 protein expression (Fig. 2C). These results indicate that Compound Y may promote neuronal differentiation in neuroblastoma cells, while THB showed a more modest effect.

3-3 Compound Y and THB enhance *GAP43* promoter activity in SK-N-SH cells

To facilitate the identification of differentiation-inducing agents for the treatment of neuroblastoma, a luciferase reporter system driven by the *GAP43* promoter was established (Fig. 3A). To validate the functionality of this system, SK-N-SH cells were transfected with the constructed luciferase plasmid and subsequently treated with retinoic acid (RA), a well-established differentiation-inducing agent. The results demonstrated that luciferase activity was significantly elevated in cells transfected with the *GAP43* promoter construct, and RA treatment further enhanced this signal (Fig. 3B). Drug screening revealed that both Compound Y and THB significantly increased *GAP43* promoter activity (Fig. 3C), consistent with previous findings on their ability to upregulate differentiation markers (Fig. 2). These findings confirm the differentiation-inducing capacity of Compound Y and THB and demonstrate the utility of the luciferase

doi:10.6342/NTU202501007

system for high-throughput screening of differentiation-inducing compounds in neuroblastoma.

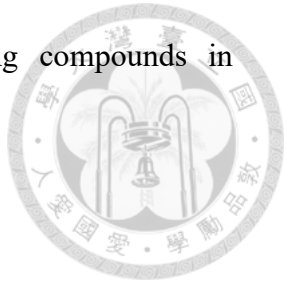

3-4 Compound Y inhibits proliferation of primary neuroblastoma cells

Before conducting *in vivo* experiments, an *ex vivo* model using primary tumor cells isolated from TH-MYCN transgenic mice was employed to assess the antiproliferative effects of Compound Y and THB. The TH-MYCN mouse is a widely used model for studying neuroblastoma due to MYCN overexpression under the tyrosine hydroxylase (TH) promoter, which targets neural crest cells [57].

Given the limited number of primary cells, a Bioinspired Nanodroplet Processing (BioNDP) platform was utilized to enable high-throughput testing using minimal cell input across 81-well chips (Fig. 4A). Compound Y significantly inhibited primary neuroblastoma cell viability in a dose-dependent manner, whereas THB had no significant effect (Fig. 4B). Importantly, treatment with either Compound Y or THB did not significantly affect the viability of HEK-293 cells, indicating a degree of selectivity (Fig. 4C). These data suggest that Compound Y effectively suppresses the growth of primary neuroblastoma cells with minimal cytotoxicity to non-neuronal cells.

doi:10.6342/NTU202501007

3-5 Compound Y attenuates neuroblastoma tumor growth *in vivo*

To investigate the *in vivo* therapeutic potential of Compound Y, TH-MYCN transgenic mice were used. Tumor development was monitored via ultrasound imaging, and treatment was initiated when tumor diameter exceeded 0.5 cm. The endpoint for the study was defined as a tumor diameter reaching 1.5 cm (Fig. 5A).

Tumors in vehicle-treated mice exhibited over fivefold growth within one week, while tumors in Compound Y-treated mice grew only threefold during the same period (Fig. 5B). Tumor volumes were recorded for each group (n = 5), and growth curves were analyzed via linear regression (Fig. 6A). Analysis of the regression slope revealed that Compound Y significantly reduced tumor growth rate in TH-MYCN mice (Fig. 6B). These findings suggest that Compound Y effectively suppresses tumor progression *in vivo*.

3-6 Compound Y prolongs survival in TH-MYCN mice

To further assess the therapeutic efficacy of Compound Y, a survival study was conducted in TH-MYCN mice. Mice treated with Compound Y demonstrated significantly prolonged survival compared to vehicle-treated controls (Fig. 7A). Additionally, there was no significant difference in body weight among the treatment groups, indicating minimal systemic toxicity (Fig. 7B). Collectively, these findings

doi:10.6342/NTU202501007

highlight Compound Y as a promising therapeutic candidate for neuroblastoma, with favorable efficacy and minimal toxicity.

doi:10.6342/NTU202501007

4. Discussion

AHR is a critical ligand-activated transcription factor involved in the regulation of neuroblastoma cell differentiation [15]. Through a cell-free dioxin response assay, THB and Compound Y were identified as endogenous and exogenous AHR ligands, respectively [51]. Prior research has also shown that THB activates AHR signaling and regulates neural differentiation in zebrafish models [51]. In the present study, cell-based assays demonstrated that both Compound Y and THB promote neural differentiation in SK-N-SH and SK-N-BE neuroblastoma cells. However, proliferation assays revealed that Compound Y showed a stronger inhibitory effect than THB in both established and primary neuroblastoma cells, suggesting that Compound Y may serve as a more promising therapeutic candidate. This was a key consideration for its selection in subsequent *in vivo* experiments.

To facilitate the screening of neuroblastoma differentiation-inducing agents, a luciferase-based reporter system driven by the *GAP43* promoter was developed. While the system effectively identified compounds such as Compound Y and THB, further enhancements are necessary. Enhancing its sensitivity could improve screening efficiency. Future applications could be enhanced by the generation of stable reporter cell lines through electroporation or viral transduction of plasmids, ensuring consistent

doi:10.6342/NTU202501007

gene expression, stronger signal output, and reduced experimental variability. Such improvements would facilitate the identification of promising differentiation agents and potentially advance therapeutic strategies for neuroblastoma.

The BioNDP platform was employed using primary neuroblastoma cells prior to the initiation of animal studies. This approach confers two distinct advantages. First, the use of primary cells enables precise assessment of drug efficacy and optimal dosing, thereby reducing the dependency on animal models. Second, the minimal culture volume (200 nL) required by the BioNDP platform efficiently addresses the challenge of limited tumor cell availability. Previous studies utilizing this platform have demonstrated its capability to identify effective drug combinations that eradicated tumors and significantly improved the survival of TH-MYCN mice [53]. Thus, the BioNDP platform offers a cost-effective, customizable, and high-throughput preclinical drug screening method.

In vivo analysis demonstrated that Compound Y significantly prolonged the survival of TH-MYCN transgenic mice (Fig. 7). However, complete tumor suppression was not observed. This outcome may be caused by the distinct mechanism of action of Compound Y. Unlike conventional chemotherapeutic agents that induce direct cytotoxic effects, Compound Y primarily functions by activating AHR signaling, thereby promoting cellular differentiation. Consequently, residual proliferative

doi:10.6342/NTU202501007

activity—particularly from cancer stem cells—may limit the overall therapeutic efficacy of differentiation-based approaches. This limitation emphasizes the growing importance of combination therapies in neuroblastoma treatment. With favorable efficacy and minimal toxicity, Compound Y may serve as an ideal candidate for combination with existing clinical agents to achieve enhanced therapeutic outcomes with minimal adverse effects.

In conclusion, the current study thoroughly evaluates the therapeutic potential of Compound Y and THB in neuroblastoma. Data obtained from *in vitro*, *ex vivo*, and *in vivo* models demonstrate that Compound Y significantly inhibits tumor progression by suppressing cell proliferation and promoting neural differentiation. These findings highlight the promise of AHR-targeting compounds as novel therapeutic agents and provide a strategic foundation for future neuroblastoma treatment development.

doi:10.6342/NTU202501007

5. References

1. Polychronopoulos, P.A., Bedoya-Reina, O.C., and Johnsen, J.I. *The Neuroblastoma Microenvironment, Heterogeneity and Immunotherapeutic Approaches*. Cancers, 2024. **16**, DOI: 10.3390/cancers16101863.
2. Friedman, D.L., Kadan-Lottick, N.S., Whitton, J., Mertens, A.C., Yasui, Y., Liu, Y., . . . Strong, L.C., *Increased risk of cancer among siblings of long-term childhood cancer survivors: a report from the childhood cancer survivor study.* Cancer Epidemiol Biomarkers Prev, 2005. **14**(8): p. 1922-7.
3. Zage, P.E., Louis, C.U., and Cohn, S.L., *New aspects of neuroblastoma treatment: ASPHO 2011 symposium review.* Pediatr Blood Cancer, 2012. **58**(7): p. 1099-105.
4. Sainero-Alcolado, L., Sjoberg Bexelius, T., Santopolo, G., Yuan, Y., Liano-Pons, J., and Arsenian-Henriksson, M., *Defining neuroblastoma: From origin to precision medicine.* Neuro Oncol, 2024. **26**(12): p. 2174-2192.
5. Maris, J.M., *Recent advances in neuroblastoma.* N Engl J Med, 2010. **362**(23): p. 2202-11.
6. Qiu, B. and Matthay, K.K., *Advancing therapy for neuroblastoma.* Nat Rev Clin Oncol, 2022. **19**(8): p. 515-533.

doi:10.6342/NTU202501007

7. Irwin, M.S., Naranjo, A., Zhang, F.F., Cohn, S.L., London, W.B., Gastier-Foster, J.M., . . . Hogarty, M.D., *Revised Neuroblastoma Risk Classification System: A Report From the Children's Oncology Group.* J Clin Oncol, 2021. **39**(29): p. 3229-3241.

8. Cohn, S.L., Pearson, A.D., London, W.B., Monclair, T., Ambros, P.F., Brodeur, G.M., . . . Force, I.T., *The International Neuroblastoma Risk Group (INRG) classification system: an INRG Task Force report.* J Clin Oncol, 2009. **27**(2): p. 289-97.

9. Tonini, G.P., *Neuroblastoma: The result of multistep transformation?* 1993. **11**(4): p. 276-282.

10. Ploessl, C., Pan, A., Maples, K.T., and Lowe, D.K., *Dinutuximab: An Anti-GD2 Monoclonal Antibody for High-Risk Neuroblastoma.* Ann Pharmacother, 2016. **50**(5): p. 416-22.

11. Cohn, S.L. and Tweddle, D.A., *MYCN amplification remains prognostically strong 20 years after its "clinical debut".* European Journal of Cancer, 2004. **40**(18): p. 2639-2642.

12. Peifer, M., Hertwig, F., Roels, F., Dreidax, D., Gartlgruber, M., Menon, R., . . . Fischer, M., *Telomerase activation by genomic rearrangements in high-risk neuroblastoma.* Nature, 2015. **526**(7575): p. 700-704.

doi:10.6342/NTU202501007

13. Norris, M.D., Bordow, S.B., Marshall, G.M., Haber, P.S., Cohn, S.L., and Haber, M., *Expression of the gene for multidrug-resistance-associated protein and outcome in patients with neuroblastoma.* N Engl J Med, 1996. **334**(4): p. 231-8.

14. Jiang, R., Xue, S., and Jin, Z., *Stable knockdown of MYCN by lentivirus-based RNAi inhibits human neuroblastoma cells growth in vitro and in vivo.* Biochemical and Biophysical Research Communications, 2011. **410**(2): p. 364-370.

15. Wu, P.Y., Liao, Y.F., Juan, H.F., Huang, H.C., Wang, B.J., Lu, Y.L., . . . Lee, H., *Aryl hydrocarbon receptor downregulates MYCN expression and promotes cell differentiation of neuroblastoma.* PLoS One, 2014. **9**(2): p. e88795.

16. Bersten, D.C., Sullivan, A.E., Peet, D.J., and Whitelaw, M.L., *bHLH–PAS proteins in cancer.* Nature Reviews Cancer, 2013. **13**(12): p. 827-841.

17. Hankinson, O., *The aryl hydrocarbon receptor complex.* Annu Rev Pharmacol Toxicol, 1995. **35**: p. 307-40.

18. Gruszczyk, J., Grandvuillemin, L., Lai-Kee-Him, J., Paloni, M., Savva, C.G., Germain, P., . . . Bourguet, W., *Cryo-EM structure of the agonist-bound Hsp90-XAP2-AHR cytosolic complex.* Nat Commun, 2022. **13**(1): p. 7010.

19. Ikuta, T., Tachibana, T., Watanabe, J., Yoshida, M., Yoneda, Y., and Kawajiri,

doi:10.6342/NTU202501007

K., *Nucleocytoplasmic shuttling of the aryl hydrocarbon receptor.* J Biochem, 2000. **127**(3): p. 503-9.

20. Kazzaz, S.A., Tawil, J., and Harhaj, E.W., *The aryl hydrocarbon receptor-interacting protein in cancer and immunity: Beyond a chaperone protein for the dioxin receptor.* Journal of Biological Chemistry, 2024. **300**(4).

21. Zanger, U.M. and Schwab, M., *Cytochrome P450 enzymes in drug metabolism: regulation of gene expression, enzyme activities, and impact of genetic variation.* Pharmacol Ther, 2013. **138**(1): p. 103-41.

22. Nebert, D.W. and Karp, C.L., *Endogenous Functions of the Aryl Hydrocarbon Receptor (AHR): Intersection of Cytochrome P450 1 (CYP1)-metabolized Eicosanoids and AHR Biology.* Journal of Biological Chemistry, 2008. **283**(52): p. 36061-36065.

23. Kohle, C. and Bock, K.W., *Coordinate regulation of Phase I and II xenobiotic metabolisms by the Ah receptor and Nrf2.* Biochem Pharmacol, 2007. **73**(12): p. 1853-62.

24. Zhang, L.M., Hatzakis, E., Nichols, R.G., Hao, R.X., Correll, J., Smith, P.B., . . . Patterson, A.D., *Metabolomics Reveals that Aryl Hydrocarbon Receptor Activation by Environmental Chemicals Induces Systemic Metabolic Dysfunction in Mice.* Environmental Science & Technology, 2015. **49**(13): p.

doi:10.6342/NTU202501007

8067-8077.

25. Kimura, A., Naka, T., Nohara, K., Fujii-Kuriyama, Y., and Kishimoto, T., *Aryl hydrocarbon receptor regulates Stat1 activation and participates in the development of Th17 cells.* Proceedings of the National Academy of Sciences, 2008. **105**(28): p. 9721-9726.

26. Kimura, A., Naka, T., Nakahama, T., Chinen, I., Masuda, K., Nohara, K., . . . Kishimoto, T., *Aryl hydrocarbon receptor in combination with Stat1 regulates LPS-induced inflammatory responses.* Journal of Experimental Medicine, 2009. **206**(9): p. 2027-2035.

27. Amit, I., Garber, M., Chevrier, N., Leite, A.P., Donner, Y., Eisenhaure, T., . . . Regev, A., *Unbiased Reconstruction of a Mammalian Transcriptional Network Mediating Pathogen Responses.* Science, 2009. **326**(5950): p. 257-263.

28. Stockinger, B., Meglio, P.D., Gialitakis, M., and Duarte, J.H., *The Aryl Hydrocarbon Receptor: Multitasking in the Immune System.* 2014. **32**(Volume 32, 2014): p. 403-432.

29. Fu, J., Nogueira, S.V., Drongelen, V.v., Coit, P., Ling, S., Rosloniec, E.F., . . . Holoshitz, J., *Shared epitope–aryl hydrocarbon receptor crosstalk underlies the mechanism of gene–environment interaction in autoimmune arthritis.* Proceedings of the National Academy of Sciences, 2018. **115**(18): p. 4755-

doi:10.6342/NTU202501007

4760.

30. Abdullah, A., Maged, M., Hairul-Islam M, I., Osama I, A., Maha, H., Manal, A., and Hamza, H., *Activation of aryl hydrocarbon receptor signaling by a novel agonist ameliorates autoimmune encephalomyelitis.* PLOS ONE, 2019. **14**(4): p. e0215981.

31. He, C.-X., Prevot, N., Boitard, C., Avner, P., and Rogner, U.C., *Inhibition of type 1 diabetes by upregulation of the circadian rhythm-related aryl hydrocarbon receptor nuclear translocator-like 2.* Immunogenetics, 2010. **62**(9): p. 585-592.

32. Marlowe, J.L., Fan, Y., Chang, X., Peng, L., Knudsen, E.S., Xia, Y., and Puga, A., *The aryl hydrocarbon receptor binds to E2F1 and inhibits E2F1-induced apoptosis.* Mol Biol Cell, 2008. **19**(8): p. 3263-71.

33. Chang, F., Wang, L., Kim, Y., Kim, M., Lee, S., and Lee, S.-w. *The Aryl Hydrocarbon Receptor Regulates Invasiveness and Motility in Acute Myeloid Leukemia Cells through Expressional Regulation of Non-Muscle Myosin Heavy Chain IIA*. International Journal of Molecular Sciences, 2024. **25**, DOI: 10.3390/ijms25158147.

34. Contador-Troca, M., Alvarez-Barrientos, A., Barrasa, E., Rico-Leo, E.M., Catalina-Fernández, I., Menacho-Márquez, M., . . . Fernández-Salguero, P.M.,

doi:10.6342/NTU202501007

The dioxin receptor has tumor suppressor activity in melanoma growth and metastasis. Carcinogenesis, 2013. **34**(12): p. 2683-2693.

35. Jin, D.Q., Jung, J.W., Lee, Y.S., and Kim, J.A., *2,3,7,8-Tetrachlorodibenzo-p-dioxin inhibits cell proliferation through arylhydrocarbon receptor-mediated G1 arrest in SK-N-SH human neuronal cells.* Neurosci Lett, 2004. **363**(1): p. 69-72.

36. Williamson, M.A., Gasiewicz, T.A., and Opanashuk, L.A., *Aryl hydrocarbon receptor expression and activity in cerebellar granule neuroblasts: implications for development and dioxin neurotoxicity.* Toxicol Sci, 2005. **83**(2): p. 340-8.

37. Dever, D.P., Adham, Z.O., Thompson, B., Genestine, M., Cherry, J., Olschowka, J.A., . . . Opanashuk, L.A., *Aryl hydrocarbon receptor deletion in cerebellar granule neuron precursors impairs neurogenesis.* Dev Neurobiol, 2016. **76**(5): p. 533-50.

38. Latchney, S.E., Hein, A.M., O'Banion, M.K., DiCicco-Bloom, E., and Opanashuk, L.A., *Deletion or activation of the aryl hydrocarbon receptor alters adult hippocampal neurogenesis and contextual fear memory.* J Neurochem, 2013. **125**(3): p. 430-45.

39. Akahoshi, E., Yoshimura, S., and Ishihara-Sugano, M., *Over-expression of*

doi:10.6342/NTU202501007

AhR (aryl hydrocarbon receptor) induces neural differentiation of Neuro2a cells: neurotoxicology study. Environ Health, 2006. **5**: p. 24.

40. Opitz, C.A., Litzenburger, U.M., Sahm, F., Ott, M., Tritschler, I., Trump, S., . . . Platten, M., *An endogenous tumour-promoting ligand of the human aryl hydrocarbon receptor.* Nature, 2011. **478**(7368): p. 197-203.

41. Wu, P.Y., Yu, I.S., Lin, Y.C., Chang, Y.T., Chen, C.C., Lin, K.H., . . . Lee, H., *Activation of Aryl Hydrocarbon Receptor by Kynurenine Impairs Progression and Metastasis of Neuroblastoma.* Cancer Res, 2019. **79**(21): p. 5550-5562.

42. Wang, W.-D., Wang, Y., Wen, H.-J., Buhler, D.R., and Hu, C.-H., *Phenylthiourea as a weak activator of aryl hydrocarbon receptor inhibiting 2,3,7,8-tetrachlorodibenzo-p-dioxin-induced CYP1A1 transcription in zebrafish embryo.* Biochemical Pharmacology, 2004. **68**(1): p. 63-71.

43. Nuti, R., Gargaro, M., Matino, D., Dolciami, D., Grohmann, U., Puccetti, P., . . . Macchiarulo, A., *Ligand binding and functional selectivity of L-tryptophan metabolites at the mouse aryl hydrocarbon receptor (mAhR).* J Chem Inf Model, 2014. **54**(12): p. 3373-83.

44. Wang, B.J., Wu, P.Y., Lu, Y.C., Chang, C.H., Lin, Y.C., Tsai, T.C., . . . Lee, H., *Establishment of a cell-free bioassay for detecting dioxin-like compounds.* Toxicol Mech Methods, 2013. **23**(6): p. 464-70.

doi:10.6342/NTU202501007

45. Brunton, P.J., Russell, J.A., and Hirst, J.J., *Allopregnanolone in the brain: protecting pregnancy and birth outcomes.* Prog Neurobiol, 2014. **113**: p. 106-36.

46. Kelleher, M.A., Hirst, J.J., and Palliser, H.K., *Changes in neuroactive steroid concentrations after preterm delivery in the Guinea pig.* Reprod Sci, 2013. **20**(11): p. 1365-75.

47. Jenkins, S.I., Pickard, M.R., Khong, M., Smith, H.L., Mann, C.L., Emes, R.D., and Chari, D.M., *Identifying the cellular targets of drug action in the central nervous system following corticosteroid therapy.* ACS Chem Neurosci, 2014. **5**(1): p. 51-63.

48. Melcangi, R.C., Giatti, S., and Garcia-Segura, L.M., *Levels and actions of neuroactive steroids in the nervous system under physiological and pathological conditions: Sex-specific features.* Neurosci Biobehav Rev, 2016. **67**: p. 25-40.

49. Pelletier, G., *Steroidogenic enzymes in the brain: morphological aspects.* Prog Brain Res, 2010. **181**: p. 193-207.

50. Diotel, N., Do Rego, J.L., Anglade, I., Vaillant, C., Pellegrini, E., Vaudry, H., and Kah, O., *The brain of teleost fish, a source, and a target of sexual steroids.* Front Neurosci, 2011. **5**: p. 137.

doi:10.6342/NTU202501007

51. Wu, P.Y., Chuang, P.Y., Chang, G.D., Chan, Y.Y., Tsai, T.C., Wang, B.J., . . . Lee, H., *Novel Endogenous Ligands of Aryl Hydrocarbon Receptor Mediate Neural Development and Differentiation of Neuroblastoma.* ACS Chem Neurosci, 2019. **10**(9): p. 4031-4042.

52. Kuo, C.T., Wang, J.Y., Lu, S.R., Lai, Y.S., Chang, H.H., Hsieh, J.T., . . . Lee, H., *A nanodroplet cell processing platform facilitating drug synergy evaluations for anti-cancer treatments.* Sci Rep, 2019. **9**(1): p. 10120.

53. Liao, Y.-T., Yu, Z.-K., Huang, Y.-X., Lin, K.-H., Kuo, C.-T., Yang, T.-S., . . . Lee, H., *Synergistic drug combination screening using a nanodroplet processing platform to enhance neuroblastoma treatment in TH-MYCN transgenic mice.* Bioengineering & Translational Medicine, 2025. **n/a**(n/a): p. e70007.

54. Tomayko, M.M. and Reynolds, C.P., *Determination of subcutaneous tumor size in athymic (nude) mice.* (0344-5704 (Print)).

55. Chung, D., Shum, A., and Caraveo, G., *GAP-43 and BASP1 in Axon Regeneration: Implications for the Treatment of Neurodegenerative Diseases.* Front Cell Dev Biol, 2020. **8**: p. 567537.

56. Schmechel, D.E., Brightman, M.W., and Marangos, P.J., *Neurons switch from non-neuronal enolase to neuron-specific enolase during differentiation.* Brain

doi:10.6342/NTU202501007

Research, 1980. **190**(1): p. 195-214.

57. Chen, L., Esfandiari, A., Reaves, W., Vu, A., Hogarty, M.D., Lunec, J., and Tweddle, D.A., *Characterisation of the p53 pathway in cell lines established from TH-MYCN transgenic mouse tumours.* Int J Oncol, 2018. **52**(3): p. 967-977.

doi:10.6342/NTU202501007

6. Figures

Figure 1

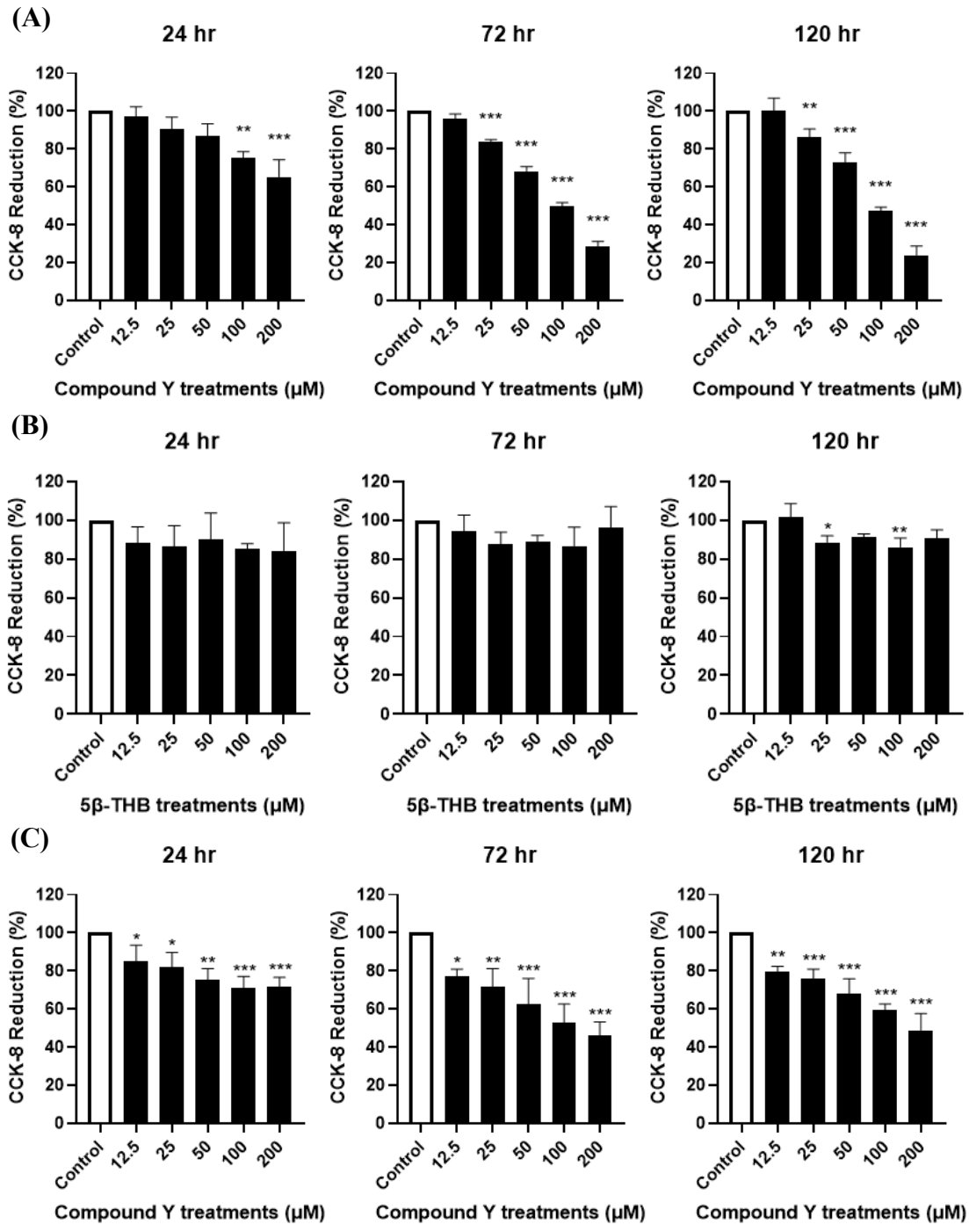

doi:10.6342/NTU202501007

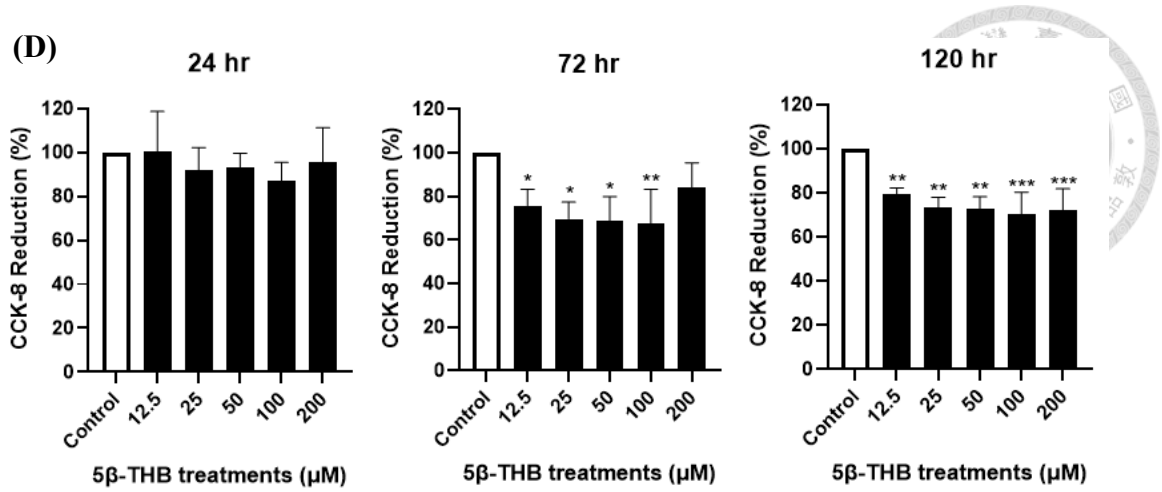

Figure 1. Compound Y and THB inhibit cell proliferation in neuroblastoma cells.

(A) SK-N-SH cells were treated with the indicated concentration of Compound Y for 24, 72, and 120 hours. (B) SK-N-SH cells were treated with the indicated concentration of THB for 24, 72, and 120 hours. (C) SK-N-BE cells were treated with the indicated concentration of Compound Y for 24, 72, and 120 hours. (D) SK-N-BE cells were treated with the indicated concentration of THB for 24, 72, and 120 hours. Cell proliferation was assessed using CCK-8 proliferation assay. The proliferation of drug-treated cells was compared to that of vehicle-treated cells. Data are presented as the mean ± SD from at least three independent experiments and analyzed by one-way ANOVA; *$p < 0.05$, **$p < 0.01$, ***$p < 0.001$.

doi:10.6342/NTU202501007

Figure 2

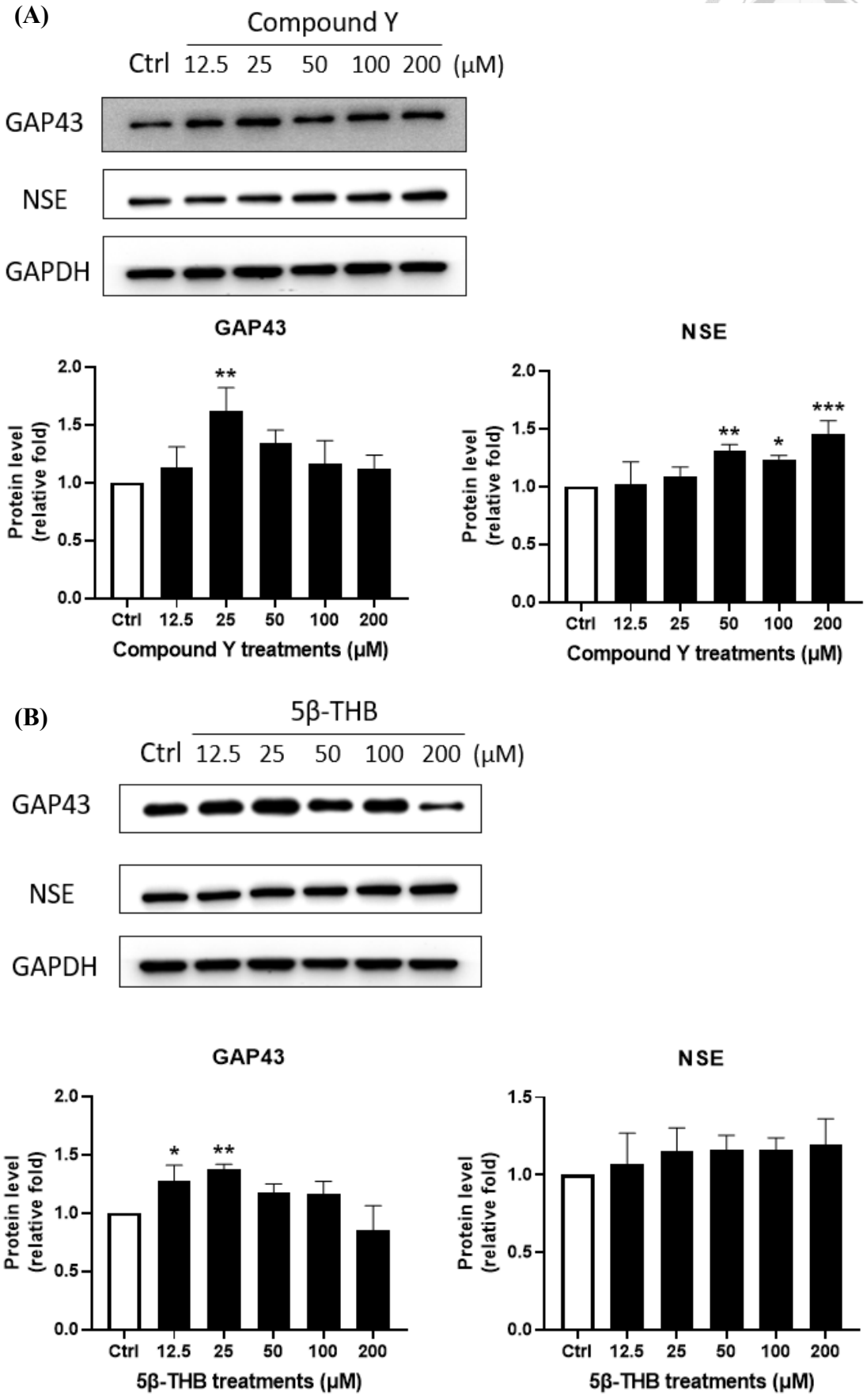

doi:10.6342/NTU202501007

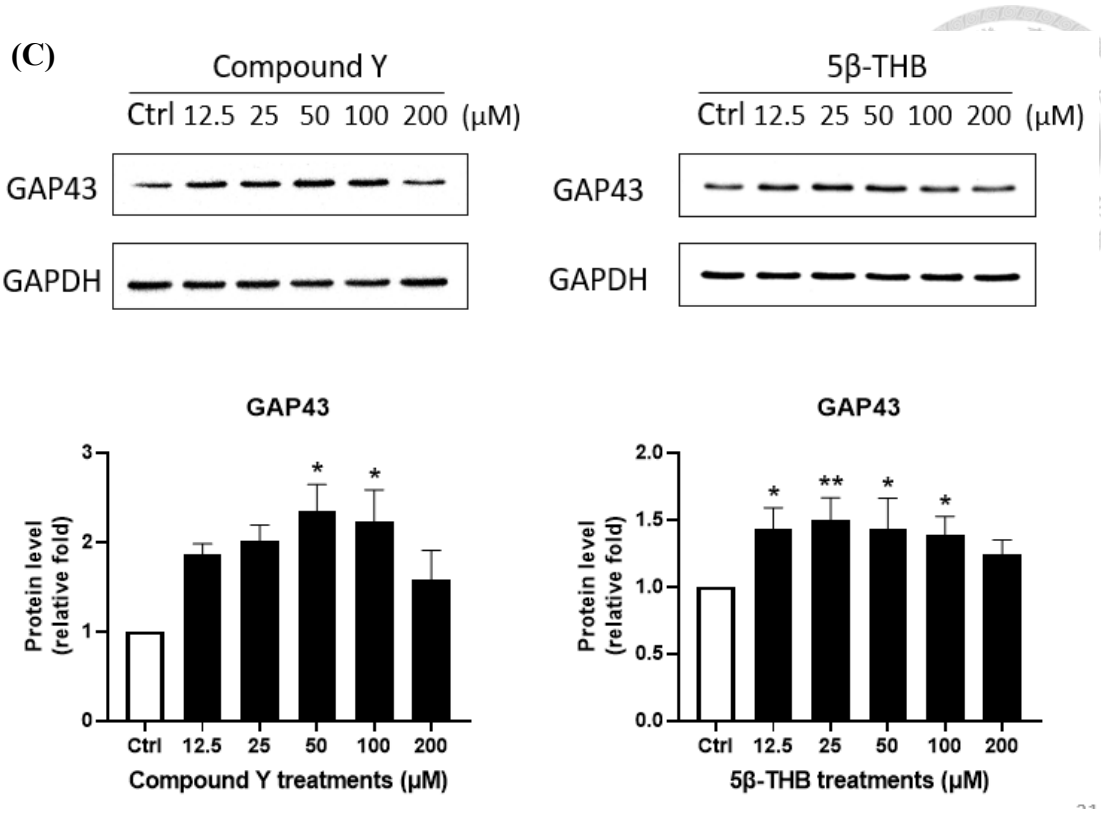

Figure 2. Compound Y and THB induce neuronal differentiation in neuroblastoma cells. (A) SK-N-SH cells were treated with the indicated concentration of Compound Y or (B) THB. The protein levels of GAP43 and NSE were assessed using Western blot. The protein levels of drug-treated cells were compared to those of vehicle-treated cells. (C) SK-N-BE cells were treated with the indicated concentration of Compound Y or THB. The protein levels of GAP43 were assessed using Western blot. The protein levels of drug-treated cells were compared to those of vehicle-treated cells. Data are presented as the mean ± SD from at least three independent experiments and analyzed by one-way ANOVA; *$p < 0.05$, **$p < 0.01$, ***$p < 0.001$.

doi:10.6342/NTU202501007

Figure 3

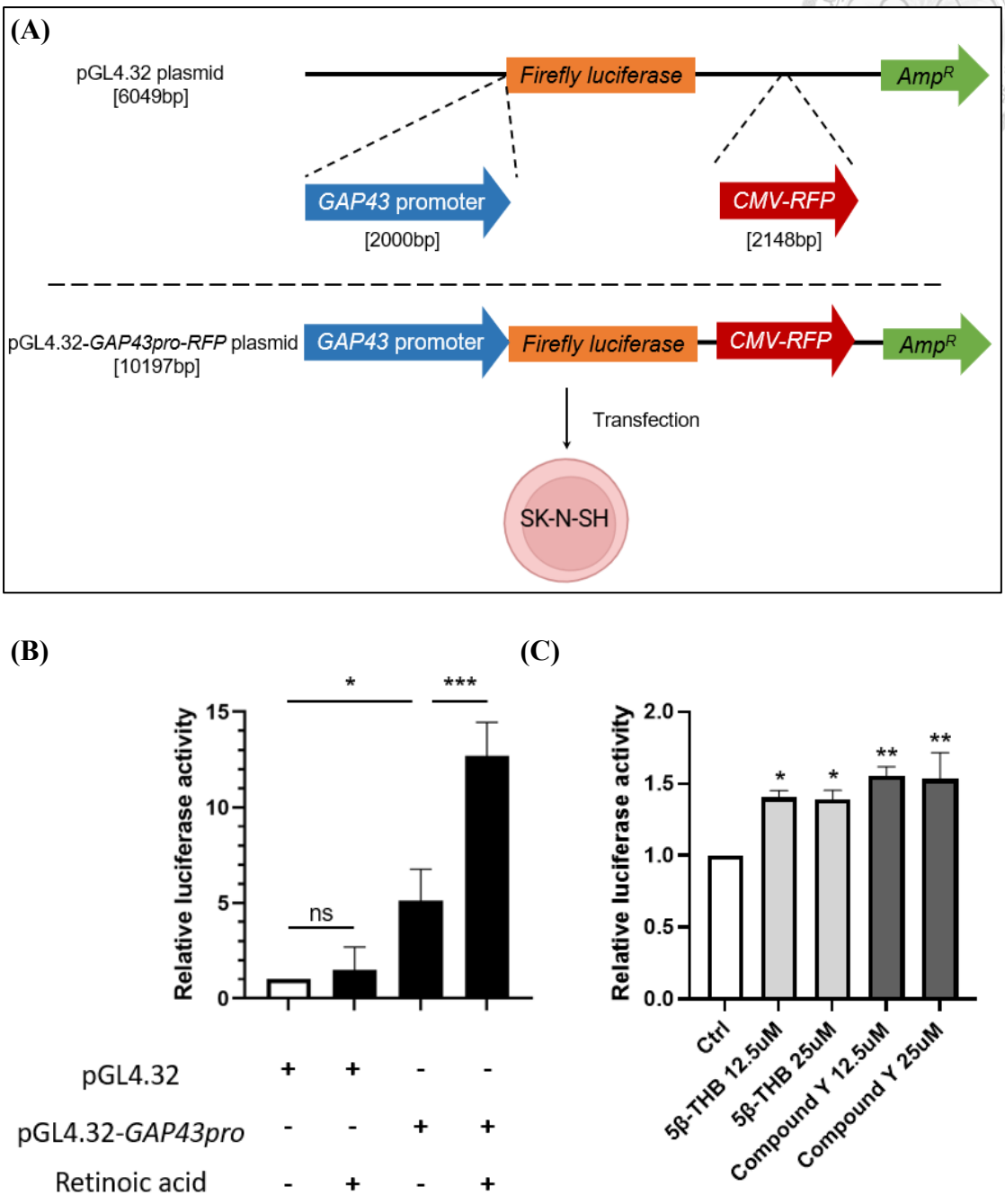

Figure 3. Compound Y and THB enhance *GAP43* promoter activity in SK-N-SH cells. (A) A DNA construct containing the *GAP43* promoter and an RFP reporter sequence was used, with RFP serving as a control for transfection efficiency. (B) Luciferase activity in SK-N-SH cells transfected with plasmids either with or without

doi:10.6342/NTU202501007

GAP43 promoter. Retinoic acid was used as a positive control. (C) Luciferase activity in SK-N-SH cells transfected with plasmid and subsequently treated with the indicated concentrations of Compound Y or THB. Data are presented as the mean ± SD from at least three independent experiments and analyzed by one-way ANOVA; *p < 0.05, **p < 0.01, ***p < 0.001.

doi:10.6342/NTU202501007

Figure 4

(A)

(B)

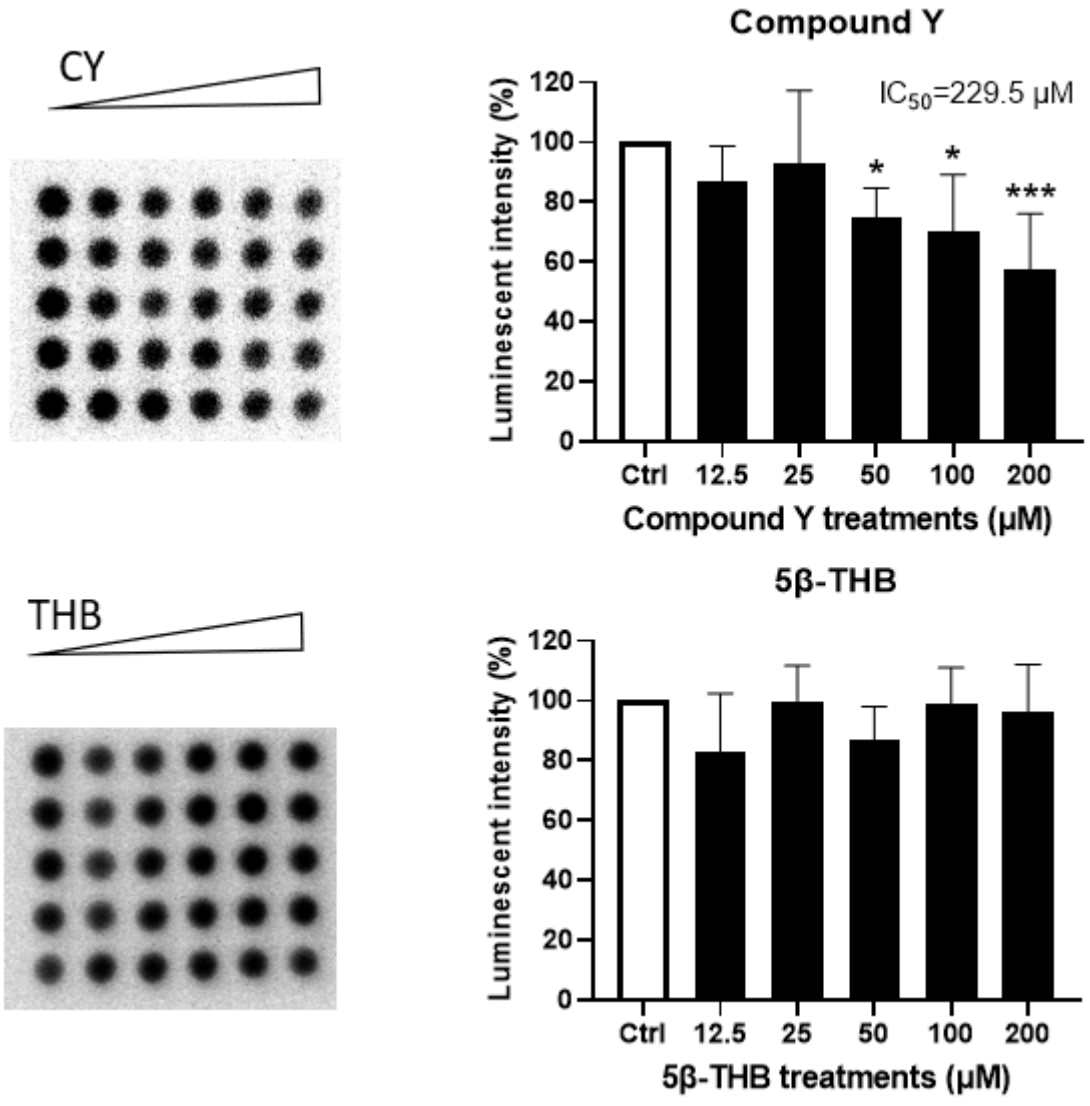

doi:10.6342/NTU202501007

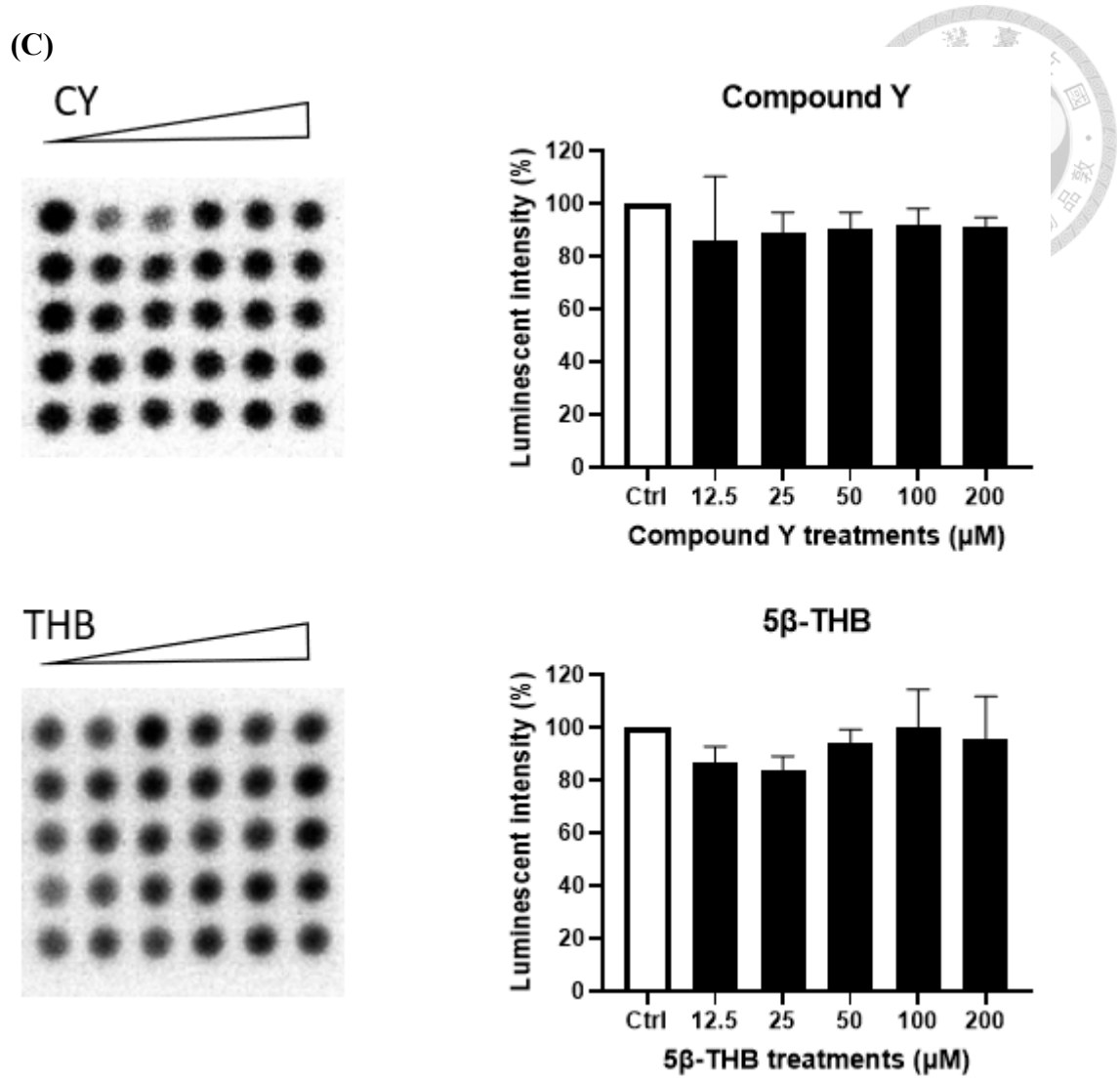

Figure 4. Compound Y inhibits proliferation of primary neuroblastoma cells. (A) Cells and the specified drugs were treated on 81-well chips through BioNDP platform. (B) Primary neuroblastoma cells were treated with the indicated concentration of Compound Y or THB for 24 hours. (C) HEK-293 cells were treated with the indicated concentration of Compound Y or THB for 24 hours. Luminescence detection was assessed using CellTiter-Glo luminescent assay. The proliferation of drug-treated cells was compared to that of vehicle-treated cells. Data are presented as the mean ± SD from

doi:10.6342/NTU202501007

at least three independent experiments and analyzed by one-way ANOVA; *$p < 0.05$, **$p < 0.01$, ***$p < 0.001$.

doi:10.6342/NTU202501007

Figure 5

(A)

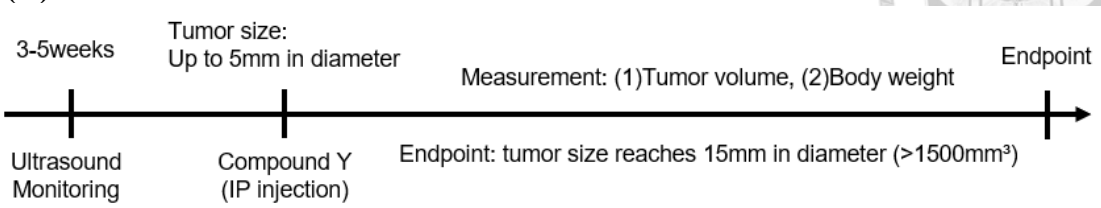

(B)

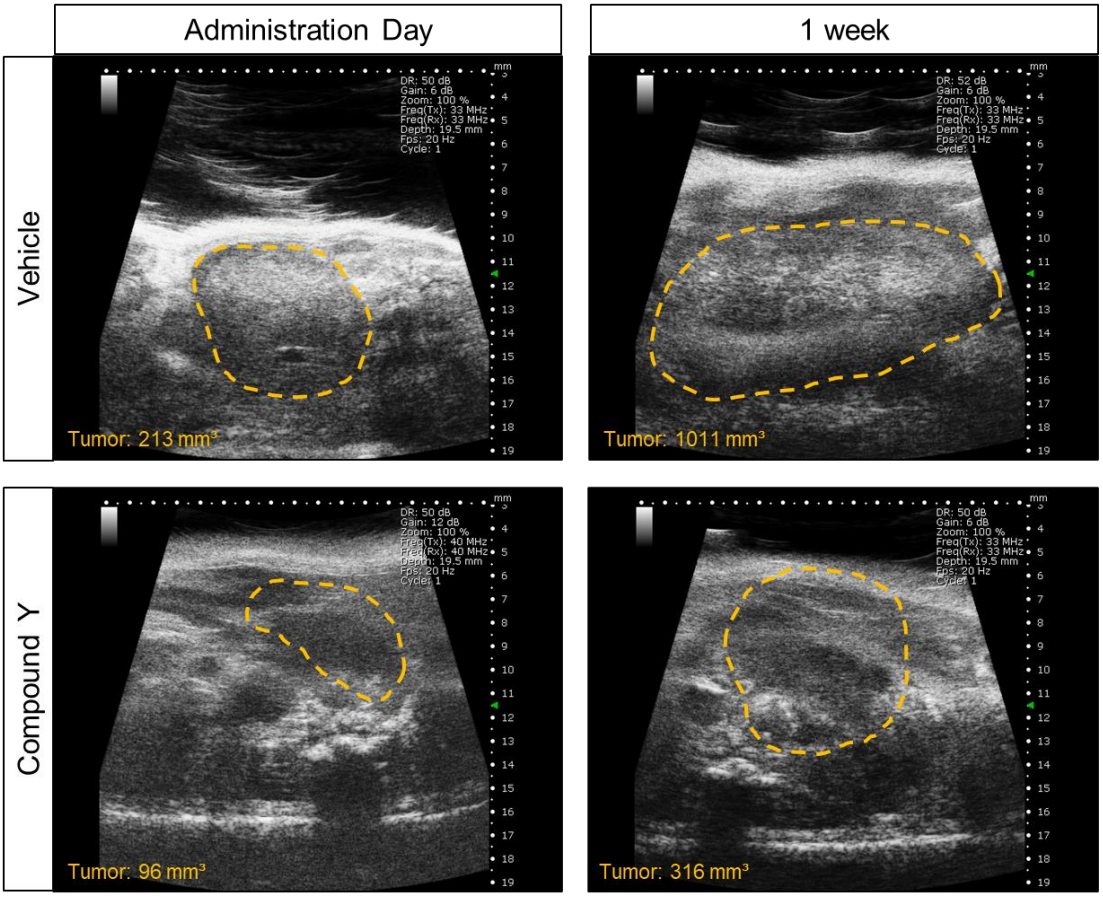

doi:10.6342/NTU202501007

Figure 5. Ultrasound imaging of TH-MYCN mice tumors. (A) Mice with abdominal tumors larger than 0.5 cm in diameter were selected for treatment. These mice were randomly assigned to receive intraperitoneal injections of either a vehicle control or Compound Y (5 mg/kg). Tumor growth was monitored via ultrasound once a week until tumor diameter reached 1.5 cm. (B) The TH-MYCN mice were administered either a vehicle control or Compound Y. The sonograms captured ventral views of the mice before treatment and after one week of treatment.

doi:10.6342/NTU202501007

Figure 6

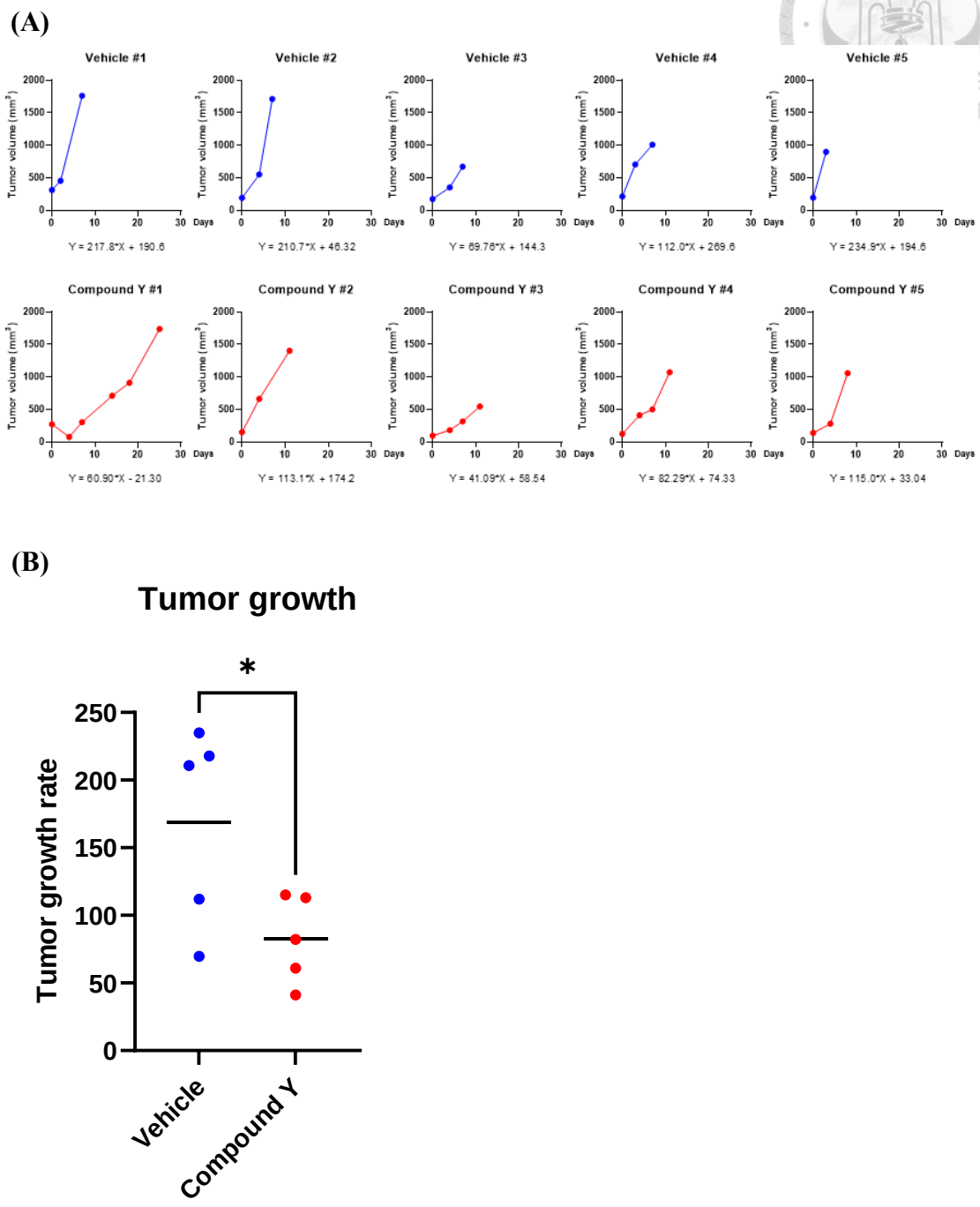

Figure 6. Compound Y attenuates neuroblastoma tumor growth. (A) The TH-MYCN mice were administered either a vehicle control or Compound Y. Tumor growth curves for the TH-MYCN mice receiving these treatments were generated. The formula for the regression line of the growth rate was calculated and is recorded below. The

doi:10.6342/NTU202501007

slope of the regression line represents the rate of tumor growth in each mouse. Tumor volume was calculated using dimensions (width, depth, and height) obtained from sonograms, based on a previously established formula [54]. (B) The tumor growth rate of drug-treated cells was compared to that of vehicle-treated cells. Student's t-test; *$p<0.05$.

doi:10.6342/NTU202501007

Figure 7

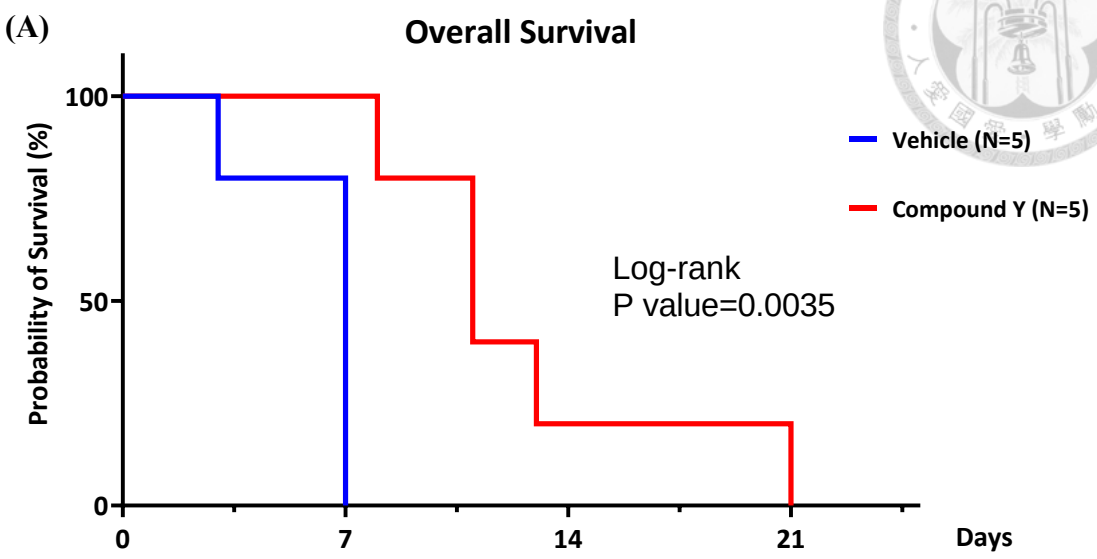

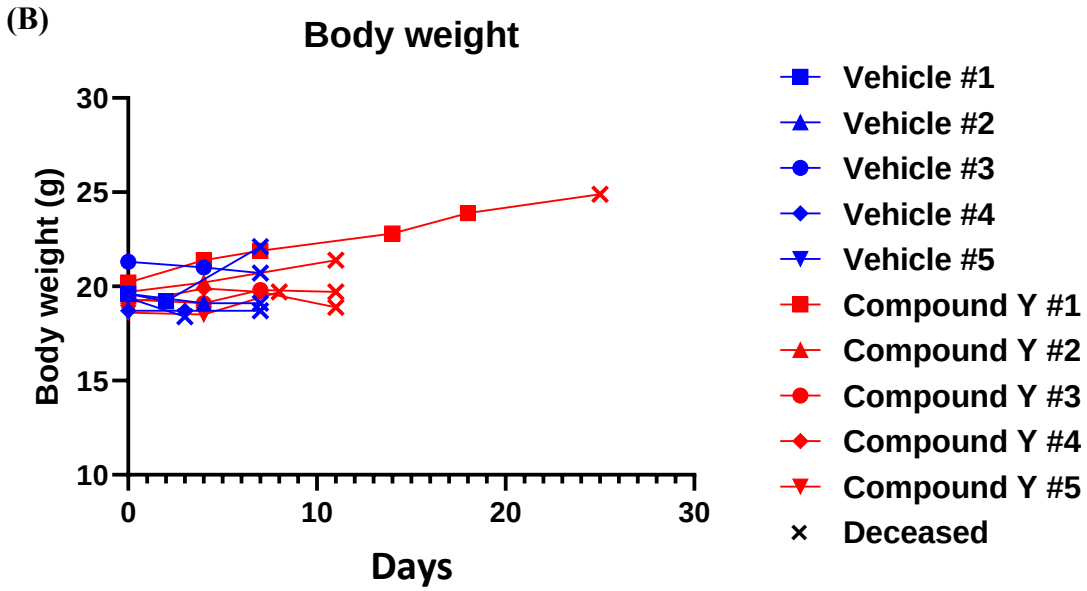

doi:10.6342/NTU202501007

Figure 7. Compound Y prolongs survival of TH-MYCN mice. (A) Survival curves for the TH-MYCN mice subjected to the indicated treatments were generated using Kaplan-Meier survival analysis. These curves illustrate the survival rates of each TH-MYCN mouse, with statistical analysis conducted using the log-rank test (Mantel-Cox method) via GraphPad Prism 9.0.0 software (***$P < 0.001$, $n = 5$ for each group). (B) The body weight of each mouse was monitored once per week ($n = 5$ for each group).

doi:10.6342/NTU202501007